Stability and performance of the SIPG and IIPG finite-element methods for wave propagation

Elena Zhebel, Shell Global Solutions International B.V., Sara Minisini, Shell Global Solutions International B.V., Alexey Kononov, Source Contracting, Wim Mulder, Shell Global Solutions International B.V. and Delft University of Technology*

SUMMARY

We consider two types of the interior penalty discontinuous Galerkin methods for wave propagation modeling: the symmetric interior penalty method (SIPG) and the incomplete interior penalty method (IIPG). The stability limit for explicit time stepping depends on the penalty parameter that imposes the continuity of the solution. For a given value of the penalty parameter, SIPG has a smaller stability limit and therefore requires smaller time steps than IIPG. IIPG, however, allows for a penalty term that is twice smaller than needed for SIPG, which results in a larger stability limit. In addition, IIPG requires less computations for the fluxes than SIPG. Numerical experiments show that this has the net effect of IIPG being more efficient than SIPG when considering the computational time required to obtain a solution with a given accuracy.

INTRODUCTION

The finite-element method is gaining popularity as an alternative to the finite-difference method for modelling wave propagation in the time domain. Finite-difference methods loose accuracy near sharp interfaces for two reasons. The representation of dipped interfaces on a finite-difference grid may lead to so-called staircasing, because parameters cannot be specified in between grid points, unless special types of discretization methods are used (Muir et al., 1992; Zhang and Liu, 2002; Hall and Wang, 2009). Also, with acoustic modeling, the pressure derivatives are not continuous across impedance contrasts with different densities, causing high-order differences to break down. With finite elements on tetrahedral meshes, the faces of elements can follow geological interfaces and topography, thereby avoiding loss of accuracy (Kononov et al., 2012). Zhebel et al. (2012) compared the finite-element method to finite differences and concluded that for very smooth models with no topography, finite differences are clearly a better choice, whereas with rough topography and complex internal structures, finite elements are more efficient in terms of the computational cost required for a given accuracy.

Earlier (Minisini et al., 2012), we compared continuous mass-lumped and discontinuous Galerkin finite elements on tetrahedral meshes and found that both methods have similar accuracy and performance. Continuous mass-lumped methods are simpler to code up but so far, only tetrahedral elements up to polynomial degree 3 have been found (Mulder, 1996; Chin-Joe-Kong et al., 1999; Zhebel et al., 2011), whereas discontinuous Galerkin finite elements do not have a formal limitation on the polynomial degree of the basis functions. Here, we focus on interior-penalty discontinuous-Galerkin (IPDG) finite elements since these offer more flexibility in mixing polynomial degrees or even mixing different discretizations. Depending on the penalty parameter, there are several variants of IPDG methods, for instance, the symmetric interior penalty method (SIPG), the incomplete interior penalty method (IIPG) and the non-symmetric interior penalty method (NIPG). Epshteyn and Rivière (2007) proved stability and convergence for elliptic problems. They provided optimal error estimates on triangular and tetrahedral meshes. De Basabe and Sen (2010) did the same for the elastic wave equation on hexahedral meshes.

Here, we investigate the stability and performance of SIPG and IIPG. First, we outline the weak formulation and discretization in space and time of those methods. Next, we provide estimates of the stability limit for time stepping as a function of the interior penalty parameter. To evaluate the computational performance, we present results for some numerical examples. The last section summarizes our conclusions.

THEORY

We consider the acoustic wave equation in three dimensions:

$$\frac{1}{c^2(x,y,z)}\frac{\partial u}{\partial t^2}-\frac{\partial^2 u}{\partial x^2}-\frac{\partial^2 u}{\partial y^2}-\frac{\partial^2 u}{\partial z^2}=s(x,y,z,t), \qquad (1)$$

where u denotes pressure at position $(x,y,z)\in\Omega$ and time $t\in[0,T]$, $c(x,y,z)$ is the velocity of the medium and $s(x,y,z,t)$ represents the source. Usually, free-surface or Dirichlet boundary conditions are given on the part of the computational domain Ω that corresponds to the boundary between the medium and the air, whereas absorbing boundary conditions are used elsewhere. Since topography and internal complex interfaces have to be accurately described, the computational domain Ω is partitioned into tetrahedral elements that should follow sharp impedance contrasts.

To discretize the wave equation (1) with finite elements, we use the weak formulation

$$\int_\Omega \frac{1}{c^2}\frac{\partial u}{\partial t^2}\,\phi\,d\Omega+\int_\Omega \nabla u\,\nabla\phi\,d\Omega-\int_{\delta\Omega}(\mathbf{n}\cdot\nabla u)\,\phi\,d\Omega = \int_\Omega s\,\phi\,d\Omega, \qquad (2)$$

for all test functions ϕ that are chosen as polynomials up to degree p. Here, $\mathbf{n}$ denotes the outward normal and $\delta\Omega$ consists of internal and external boundaries of the domain Ω. In case of discontinuous Galerkin finite elements, the solution is discontinuous across the internal boundaries. The term with the normal, called flux term, is given by

$$-\int_{\delta\Omega}[u]\{\nabla\phi\}\,d\Omega+\varepsilon\int_{\delta\Omega}[\phi]\{\nabla u\}\,d\Omega+\gamma\int_{\delta\Omega}[u][\phi]\,d\Omega.$$

If u^+ is the solution inside the element and u^- lives on one of the neighboring elements, then $[u]:=u^+-u^-$ denotes the

DOI http://dx.doi.org/10.1190/segam2012-0635.1

jump across the element boundary and $\{u\} := \frac{1}{2}(u^+ + u^-)$ is the average, whereas γ is a penalty parameter. Different values of the parameters ε and γ define different variants of the finite-element discretization. Here, we only consider two of them:

- the Symmetric Interior Penalty method (SIPG) with $\varepsilon = -1$ and $\gamma > 0$,
- the Incomplete Interior Penalty method (IIPG) with $\varepsilon = 0$ and $\gamma > 0$.

We refer to (Rivière, 2008) for an overview of other variants.

If we express the solution in the basis of the test functions, $u(x,y,z,t) = \sum u_j(t)\phi_j(x,y,z)$, then the flux term for a face F for each element is given by

$$\begin{aligned}
&-\tfrac{1}{2}\int_F (\nabla\phi_j\cdot\mathbf{n})^+\phi_i^+ u_j^+ ds - \tfrac{1}{2}\int_F (\nabla\phi_j\cdot\mathbf{n})^-\phi_i^+ u_j^- ds \\
&+\tfrac{\varepsilon}{2}\int_F (\nabla\phi_i\cdot\mathbf{n})^+\phi_j^+ u_j^+ ds - \tfrac{\varepsilon}{2}\int_F (\nabla\phi_i\cdot\mathbf{n})^+\phi_j^- u_j^- ds \\
&+\gamma\int_F u_j^+\phi_j^+\phi_i^+ ds - \gamma\int_F u_j^-\phi_j^-\phi_i^+ ds \\
&=: (A_{ij}+\varepsilon B_{ij}+\gamma C_{ij})u_j^+ + (D_{ij}+\varepsilon E_{ij}+\gamma F_{ij})u_j^- .
\end{aligned}$$

Note that SIPG has $\varepsilon = -1$ and requires computation of two extra matrices per face for each element compared to IIPG with $\varepsilon = 0$.

Discretizing the weak formulation (2), we obtain for each element

$$\mathbf{M}\mathbf{u}_{tt} + \mathbf{K}\mathbf{u} + \mathbf{F}^+\mathbf{u} + \mathbf{F}^-\mathbf{u}^- = \mathbf{s},$$

where $\mathbf{M}$ and $\mathbf{K}$ are the local mass and stiffness matrix, respectively. We also have the contribution of the fluxes. The term $\mathbf{F}^+$ denotes the sum of outgoing fluxes over the four faces in the given element. The second term $\mathbf{F}^-$ contains incoming fluxes from the four neighboring elements.

By choosing a symmetric time-marching scheme, for example leapfrog, we obtain a fully algebraic system for each element of the form

$$\mathbf{u}_{n+1} = 2\mathbf{u}_n - \mathbf{u}_{n-1} + \Delta t^2\,\mathbf{M}^{-1}\left(-\mathbf{K}\mathbf{u}_n - \mathbf{F}^+\mathbf{u}_n - \mathbf{F}^-\mathbf{u}_n^- + \mathbf{s}_n\right).$$

The only unknown is the vector $\mathbf{u}_{n+1}$. The values of the solution at the previous time steps n and $n-1$ are known. The generalization to higher-order time stepping is straightforward and involves the repeated application of the spatial operator on the solution at time step n (Dablain, 1986).

STABILITY

The stability condition for time stepping is expressed as

$$\Delta t \le \mathtt{CFL}(d/c)_{\min},$$

where $(d/c)_{\min}$ is the minimum over all elements of the ratio of the diameter of the inscribed sphere and the velocity c per element. The Courant-Friedrichs-Lewy number (Courant et al., 1928) can be taken as $\mathtt{CFL} = 2/(d\sqrt{\rho_s})$, using the spectral radius ρ_s of the spatial operator and the largest diameter d of the inscribed spheres of the elements. For higher-order time stepping, CFL has to be multiplied by a constant factor, for instance, by $\sqrt{3} = 1.73$ for fourth-order time stepping (Dablain, 1986).

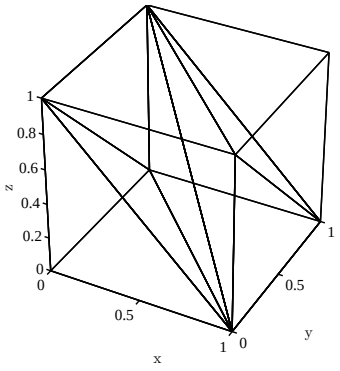

Figure 1: Unit cube with 6 tetrahedra used for estimating the time-stepping stability limits of the finite-element discretizations.

To estimate the spectral radius, we performed Fourier stability analysis on the unit cube packed with 6 tetrahedra, shown in Figure 1, which is periodically extended in the 3 coordinates. We then constructed the matrix $\mathbf{L} = \mathbf{M}^{-1}(\mathbf{K} + \mathbf{F}^+ + \mathbf{F}^-)$ corresponding to the spatial operator by running our finite-element code on a configuration of $3^3 = 27$ unit cubes on the domain $[-1,2]^3$ with unit velocity and assembled the matrix $\mathbf{L}$ for that case. For continuous elements, we would have to select a subset of nodes in the domain $[0,1)^3$ with degrees of freedom that can be arranged in a vector $\mathbf{v}$. With shift operators T_j, $j = 1,2,3$ in the x-, y-, and z-direction, respectively, over a unit distance, we would then express all other degrees of freedom into those of $\mathbf{v}$. For the discontinuous elements of polynomial degree p considered here, the vector $\mathbf{v}$ consists of all $(1+p)(2+p)(3+p)/6$ degrees of freedom inside the domain $(0,1)^3$, placing nodes on faces, edges, and vertices just inside the element. After a spatial Fourier transform, the symbol of the shift operator becomes $\hat{T}_j = \exp(\imath k_j \Delta x)$, where Δx is the grid spacing, in the present case of unit length, and k_j is the wavenumber in each coordinate direction. If we define $\xi_j = k_j\Delta x$ with $\xi_j \in (-\pi,\pi]$, then $\hat{T}_j = \exp(\imath\xi_j)$. The shift operators enable expression of the values of the degrees of freedom in the neighboring cubes in terms of those in the central one. The spectral radius ρ_s is the largest eigenvalue of the Fourier symbol of the spatial operator, $\hat{\mathbf{L}}$, over all sets of scaled wavenumbers $\{\xi_1,\xi_2,\xi_3\}$ and can be found by a numerical maximization algorithm.

Figure 2 shows the stability condition as a function of the penalty parameter γ for SIPG and IIPG methods on elements up to degree $p = 4$. For given γ, the stability limit is lower for IIPG, which can result in a larger number of time steps. At a given CFL, the SIPG method requires a larger penalty parameter than IIPG, meaning that a different penalty parameter has to be chosen for SIPG and for IIPG to preserve the same number of time steps. These estimates agree with results obtained for triangles by Agut et al. (2011).

DOI http://dx.doi.org/10.1190/segam2012-0635.1

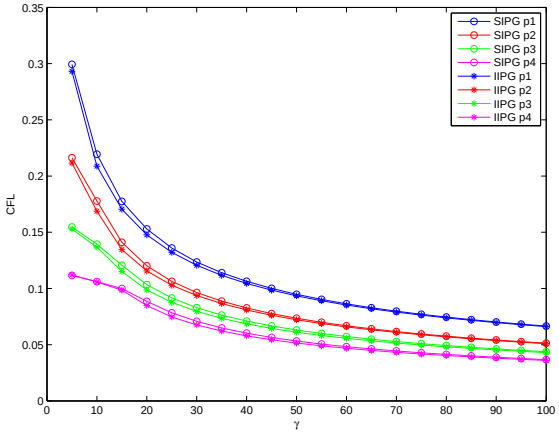

Figure 2: Time-stepping stability as a function of the penalty parameter γ.

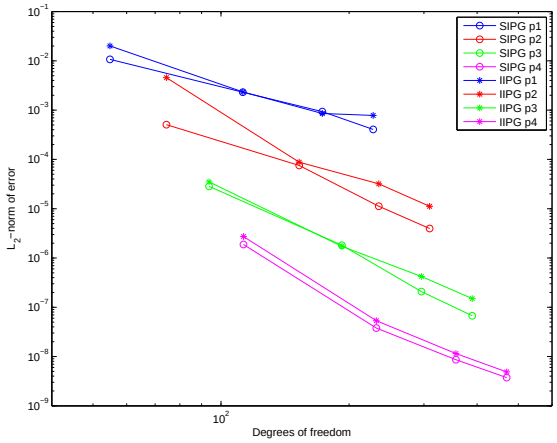

Figure 3: Absolute error as a function of degrees of freedom for SIPG and IIPG with degrees 1, 2, 3 or 4.

The question is: what is the smallest value of γ for SIPG and for IIPG that provides a stable spatial discretization? Epshteyn and Rivière (2007) have estimated a lower bound of the penalty parameter γ for SIPG in case of an elliptic problem for an interior face F in the domain:

$$\gamma_F^{\text{SIPG}} = 3p(p+2)\frac{d_{\max}\cot\theta}{A_F},$$

where $d_{\max}$ is the maximum diameter over all elements in the domain, A_F is area of the face, θ is the dihedral angle such that it gives the smallest $\sin\theta$ over all dihedral angles θ for a given element and p is degree of the element. We performed an analogous analysis for IIPG and found a lower bound of the penalty parameter

$$\gamma_F^{\text{IIPG}} = \frac{3p(p+2)}{2}\frac{d\cot\theta}{A_F} = \frac{\gamma_F^{\text{SIPG}}}{2}.$$

It can be seen from Figure 2 that, if the penalty parameter for IIPG is twice smaller than for SIPG, then the CFL of IIPG will be larger than for SIPG. Therefore, IIPG requires less time steps than SIPG. Note that we ignored the numerical error due to time stepping in this discussion.

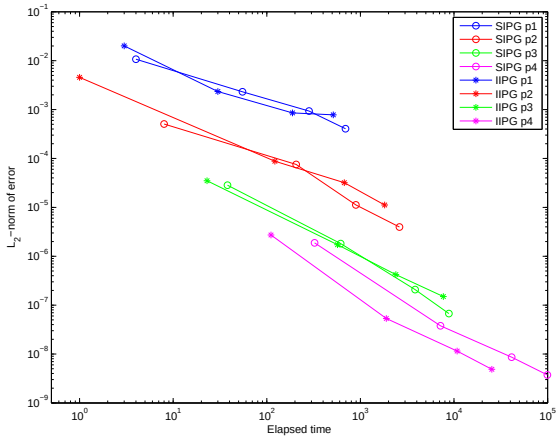

Figure 4: Absolute error as a function of computational time on 12 cores using OpenMP. To save storage, the mass, stiffness and flux matrices were recomputed in each time step.

RESULTS

To investigate the accuracy and efficiency of SIPG and IIPG, we consider a problem with a known exact solution of the constant-density constant-velocity wave equation in the three-dimensional domain $\Omega = [0,2]\times[0,2]\times[0,2]$ km^3 in the time interval $t = [0, 0.05]$ s. An exact solution is given by

$$u_{\text{exact}} = \cos(kx)\cos(kct).$$

We choose $c = 1.5$ km/s and a spatial frequency k equal to 5 half-periods over the length of the domain Ω. This problem is discretized by discontinuous Galerkin finite elements of degree $p = 1$, 2, 3 and 4 for SIPG and IIPG on a series of structured tetrahedral meshes with decreasing element sizes.

For the penalty parameter in SIPG, we choose a value far away from the stability limit to ensure the convergence: $\gamma^{\text{SIPG}} = 80$. The penalty for IIPG is chosen as $\gamma^{\text{IIPG}} = 40$. From Figure 2, we can estimate the upper bound for CFL and choose $\text{CFL}^{\text{SIPG}} = 1.0$ and $\text{CFL}^{\text{IIPG}} = 1.2$, respectively. As seen in Figure 3, IIPG has a slower convergence than SIPG. SIPG has a better convergence behavior because of its symmetry and corresponding energy conservation property. Figure 4 displays a performance comparison of SIPG and IIPG for degrees up to 4. In particular for degree $p = 4$, IIPG is several times faster than SIPG when a given accuracy should be obtained.

As a more realistic example than just a standing wave, Figure 5 shows a vertical section of a 3-D velocity model. Snapshots at 3 times are displayed in Figure 6.

DOI http://dx.doi.org/10.1190/segam2012-0635.1

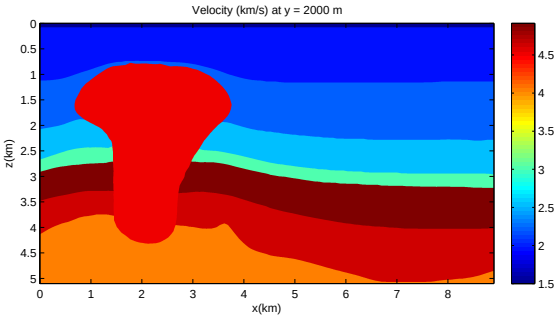

Figure 5: Vertical cross-section of a 3-D velocity model.

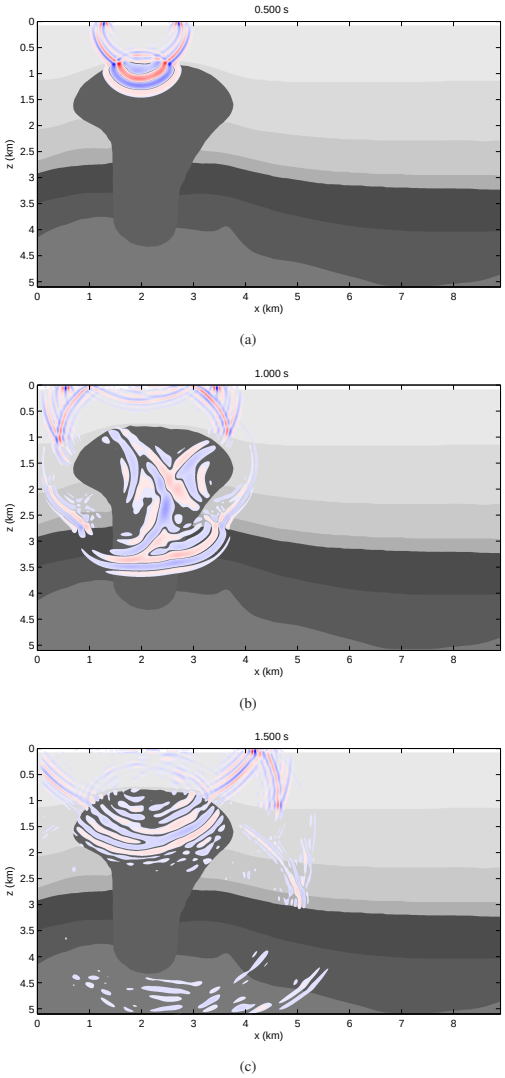

Figure 6: Snapshots of the seismic pressure wavefield in a vertical section, computed with the 3-D acoustic finite-element code, at (a) 0.5 s, (b) 1 s and (c) 1.5 s.

CONCLUSIONS

We have investigated the performance of two interior penalty methods: the symmetric interior penalty discontinuous Galerkin method (SIPG) and the incomplete interior discontinuous Galerkin method (IIPG). The two methods require a different choice of the penalty parameter, each leading to a difference stability limit for time stepping. We found that IIPG requires a smaller penalty parameter and allows for a larger time steps than SIPG. Moreover, the computational cost of the fluxes is smaller for SIPG then for IIPG. Therefore, IIPG is the preferred choice.

DOI http://dx.doi.org/10.1190/segam2012-0635.1

http://dx.doi.org/10.1190/segam2012-0635.1

EDITED REFERENCES

Note: This reference list is a copy-edited version of the reference list submitted by the author. Reference lists for the 2012 SEG Technical Program Expanded Abstracts have been copy edited so that references provided with the online metadata for each paper will achieve a high degree of linking to cited sources that appear on the Web.

REFERENCES

Agut, C., J. Bart, and J. Diaz, 2011, Numerical study of the stability of the interior penalty discontinuous Galerkin method for the wave equation with 2D triangulations: Technical Report RR-7719, INRIA.

Chin-Joe-Kong, M. J. S., W. A. Mulder, and M. van Veldhuizen, 1999, Higher-order triangular and tetrahedral finite elements with mass lumping for solving the wave equation: Journal of Engineering Mathematics, **35**, 405–426, doi: 10.1023/A:1004420829610.

Courant, R., K. Friedrichs, and H. Lewy, 1928, Über die partiellen Differenzengleichungen der mathematischen Physik: Mathematische Annalen, **100**, 32–74, doi: 10.1007/BF01448839.

Dablain, M. A., 1986, The application of high-order differencing to the scalar wave equation: Geophysics, **51**, 54–66, doi: 10.1190/1.1442040.

De Basabe, J. D., and M. K. Sen, 2010, Stability of the high-order finite elements for acoustic or elastic wave propagation with high-order time stepping: Geophysical Journal International, **181**, 577–590, doi: 10.1111/j.1365-246X.2010.04536.x.

Epshteyn, Y., and B. Rivière, 2007, Estimation of penalty parameters for symmetric interior penalty Galerkin methods: Journal of Computational and Applied Mathematics, 206, no. 2, 843–872, doi: 10.1016/j.cam.2006.08.029.

Hall, F., and Y. Wang, 2009, Elastic wave modelling by an integrated finite difference method: Geophysical Journal International, 177, no. 1, 104–114, doi: 10.1111/j.1365-246X.2008.04065.x.

Kononov, A., S. Minisini, E. Zhebel, and W. A. Mulder, 2012, A 3-D tetrahedral mesh generator for seismic problems: 74th Conference & Exhibition, EAGE, Extended Abstracts.

Minisini, S., E. Zhebel, A. Kononov, and W. A. Mulder, 2012, Efficiency comparisons for higher-order continuous mass-lumped and discontinuous Galerkin finite-element methods for the 3-D acoustic wave equation: 74th Conference & Exhibition, EAGE, Extended Abstracts.

Muir, F., J. Dellinger, J. Etgen, and D. Nichols, 1992, Modeling elastic fields across irregular boundaries: Geophysics, **57**, 1189–1193, doi: 10.1190/1.1443332.

Mulder, W. A., 1996, A comparison between higher-order finite elements and finite differences for solving the wave equation: Proceedings of the Second ECCOMAS Conference on Numerical Methods in Engineering, John Wiley & Sons, 344–350.

Rivière, B., 2008, Discontinuous Galerkin methods for solving elliptic and parabolic equations: Theory and implementation: SIAM Frontiers in Mathematics, vol. 35.

Zhang, J., and T. Liu, 2002, Elastic wave modelling in 3-D heterogeneous media: 3-D grid method: Geophysical Journal International, **150**, 780–799, doi: 10.1046/j.1365-246X.2002.01743.x.

Zhebel, E., S. Minisini, A. Kononov, and W. A. Mulder, 2011, Solving the 3D acoustic wave equation with higher-order mass-lumped tetrahedral finite elements: 73rd Conference & Exhibition, Extended Abstracts.

DOI http://dx.doi.org/10.1190/segam2012-0635.1

Zhebel, E., S. Minisini, A. Kononov, and W. A. Mulder, 2012, A comparison of continuous mass-lumped finite elements and finite differences for 3-D acoustics in the time domain: 74th Conference & Exhibition, EAGE, Extended Abstracts.

DOI http://dx.doi.org/10.1190/segam2012-0635.1